M = magma concentration, kg/m^3
n = population density, #/m^4
n^o = nuclei population density, #/m^4
N = impeller speed, s^{-1}
p = exponent
P = power input, W
P_o = power number
s = exponent
ϵ = specific power input, W/kg
μ = moment of crystal size distribution
ρ = density, kg/m^3
ρ_s = solids density, kg/m^3
τ = residence time, s
ϕ_{mv} = vapor load, kg/s
ϕ_v = volumetric flow rate, m^3/s

LITERATURE CITED

Asselbergs, C. J. and E. J. De Jong, "Some theoretical aspects of the population density distribution in a NaCl evaporating crystallizer with external circulation," Proc. 5th Symp. on Industrial Crystallization, CHISA (1972).

Bemer, G. G., "Agglomeration in suspension: A study of mechanisms and kinetics," Ph.D. Thesis, Delft University of Technology (1979).

Bujac, P. D. B., "Attrition and secondary nucleation in agitated crystal slurries," *Indus. Crystallization*, **23**, J. W. Mullin, ed. Plenum Press, New York (1976).

Evans, T. W., G. Margolis, and A. F. Sarofim, "Mechanisms of secondary nucleation in agitated crystallizers," *AIChE J.*, **20**, 950 (1974).

Garabedian, H., and R. F. Strickland-Constable, "Collision breeding of crystal nuclei: sodium chlorate," *J. Cryst. Growth.*, **13**, 506 (1972).

Grootscholten, P. A. M., C. J. Asselbergs, and E. J. De Jong, "Relevance of pilot scale research," 73rd AIChE Annual Meeting, Chicago (1980).

Johnson R. T., R. W. Rousseau, and W. L. McCabe, "Factors affecting contact nucleation," *AIChE Symp. Ser.*, **68**, 31 (1972).

Koros, W. J., D. A. Dalrymple, R. P. Kuhlman, and N. F. Brockmeier, "Crystallization of sodium chloride in a continuous mixed-suspension crystallizer," *AIChE Symp. Ser.*, **68**, 67 (1972).

Van't Land, C. M., and B. G. Wienk, "Control of particle size in industrial NaCl-crystallization," *Indus. Crystallization*, **51**, J. W. Mullin ed., Plenum Press, New York (1976).

Larson, M. A., and L. L. Bendig, "Nuclei generation from repetitive contacting," *AIChE Symp. Ser.*, **72**, 21 (1976).

Liu, Yih-An, and G. D. Botsaris, "Impurity effects in continuous-flow mixed suspension crystallizers," *AIChE J.*, **19**, 510 (1973).

Randolph, A. D., and S. K. Sikdar, "Effect of soft impeller coating on the net formation of secondary nuclei," *AIChE J.*, **20**, 410 (1974).

Rousseau, R. W., K. K. Li, and W. L. McCabe, "The influence of seed crystal size on nucleation rates," *AIChE Symp. Ser.*, **72**, 48 (1976).

Scrutton, A., "Laboratory study of the crystallization of sodium chloride from brine," 5th Symposium on Salt, Hamburg (1979).

Scrutton, A., and P. A. M. Grootscholten, "A Study on the dissolution and growth of sodium chloride crystals, *Trans. Inst. Chem. Engrs.* (Oct., 1981).

Shah, B. C., W. L. McCabe, and R. W. Rousseau, "Polyethylene vs stainless steel impellers for crystallization processes," *AIChE J.*, **19**, 194 (1973).

Tai, C. Y., W. L. McCabe, and R. W. Rousseau, "Contact nucleation of various crystal types," *AIChE J.*, **21**, 351 (1975).

Youngquist, G. R., J. Estrin, R. Jaganathan, and C. Y. Sung, "Secondary nucleation by fluid shear," 67th AIChE Annual Meeting, Washington (1974).

Manuscript received May 13, 1981; revision received October 13, and accepted October 28, 1981.

Kinetics of Thermal Regeneration Reaction of Activated Carbons used in Waste Water Treatment

The kinetics of the thermal regeneration of activated carbons used in the waste water treatment was analyzed on the basis of a model that the regeneration reaction consists of a set of many first-order reactions each of which has different activation energy and frequency factor. The frequency factors were correlated approximately by a function of the activation energy.

The difference in the activation energy was represented by a distribution curve which was obtained by analyzing the thermogravimetric curve (TG curve) measured under a constant heating rate. The weight loss during the regeneration reaction under complicated heating conditions was well predicted by use of the distribution curve determined by the proposed method. This method describing the kinetics of the thermal regeneration may be applied to the design of reactors regenerating spent carbons.

KENJI HASHIMOTO,
KOUICHI MIURA
and
TSUNEO WATANABE

Department of Chemical Engineering
Kyoto University
Kyoto, Japan

SCOPE

Activated carbons have been widely used in adsorption processes for the purpose of the removal of toxic substances, the recovery of valuable substances, the fractionation of mixtures, and so on. In recent years, advanced waste water treatment using activated carbons has received much attention. Since activated carbons are rather expensive, the spent carbons are used again and again by repeating the regeneration. Several methods such as thermal regeneration, chemical regeneration, biological regeneration, and solvent extraction have been proposed for the regeneration of spent carbons (Loven, 1973). Of these methods, thermal regeneration is by far the one most commonly used. Thermal regeneration is usually performed in

flow type reactors such as the multiple hearth furnace, the rotary kiln, and the moving bed.

The change in the properties of activated carbons, such as pore surface area, iodine number and yield, was systematically examined by several investigators (Hutchins, 1973; Kawazoe et al., 1979; Hashimoto et al., 1979). To design thermal regenerators rationally, however, the analysis of the thermal regeneration reaction is necessary. The regeneration reaction was analyzed by a few investigators (Suzuki et al., 1978; Urano, 1972) based on a single reaction model, but complicated multiple reactions are expected to occur during the regeneration of the activated carbons used in the waste water treatment.

The pyrolysis reaction of coal also consists of multiple reactions, which were analyzed by Pitt (1962) and Anthony et al. (1975) based on a model that the pyrolysis consists of many irreversible first-order reactions each of which has different activation energy. This method was first derived by Vand (1942) to account for the irreversible change in the resistance of metallic films. In those studies the frequency factors were assumed to be constant for all reactions. However, it is more rational to consider the variations in both frequency factor and activation energy.

The objectives of this paper are to develop a method for analyzing the regeneration reaction by extending the method of Vand by taking into account the variation of the frequency factor, and to examine experimentally the validity of the method.

CONCLUSIONS AND SIGNIFICANCE

The regeneration reaction of the spent activated carbons in a nitrogen atmosphere was analyzed based on a model that the regeneration reaction consists of many first-order reactions each of which has different frequency factor in addition to different activation energy. To test the validity of the model four kinds of spent activated carbons were employed as samples. Two of them were used for the treatment of the municipal waste waters, and the other two were used to purify the waste waters of chemical factories. The frequency factors were correlated by a function of the activation energy. The difference in the activation energy was represented by a distribution curve which was obtained by analyzing a thermogravimetric curve measured under a constant heating rate. By use of the distribution curve, the weight decrease of the spent carbon during the regeneration performed under complicated heating conditions was well predicted.

It was then examined whether the model could be applied to the thermal regeneration performed in an atmosphere of steam. Although the gasification of the carbonized adsorbates as well as the activated carbon itself became significant during the regeneration in the atmosphere, the method developed in this paper was successfully applicable to the regeneration reaction.

The developed method is expected to be applicable to the analysis of other complex reactions including coal gasification.

The spent carbons are gradually heated in regenerators such as the multiple hearth furnace, the rotary kiln, and the moving bed. During the heating process, the carbons pass through the zones of drying, thermal desorption, pyrolysis and carbonization (200 to 650°C), and gasification over a high temperature range (650 to 1,000°C) in the presence of limited quantities of oxidizing gas such as steam, flue gas, and oxygen (Loven, 1973). At the present time, the design of regenerators is generally based upon experience without the benefit of detailed kinetic data. For designing regenerators rationally, the kinetics during the regeneration must be studied.

Suzuki et al. (1978) classified the regeneration performed in an inert atmosphere into three types, and analyzed two of them by using single reaction models. Urano (1972) investigated the effect of oxygen pressure in the inert gas on the course of the regeneration. He also adopted a single reaction model to analyze the experimental data. However, multiple reactions are expected to occur during the regeneration of the activated carbons used in the waste water treatment because various substances are adsorbed onto the activated carbons.

Pitt (1962) and Anthony et al. (1975) analyzed the pyrolysis of coal based on a method that the pyrolysis consists of many irreversible first-order reactions each of which has different activation energy. This method was first presented by Vand (1942) to analyze the irreversible change in the resistance of metallic films prepared by evaporation. This method was applied successfully to account for the change in their experimental data, but the frequency factors, which are actually different for individual reactions, were assumed to be the same for all reactions.

In this paper the method presented by Vand has been extended by taking into account the variation in the frequency factor as well as the distribution of the activation energy. The extended method was first applied successfully to analyze the regeneration reaction performed in a nitrogen atmosphere and under a complicated heating pattern. Furthermore, it was examined whether the method was applicable to the analysis of the thermal regeneration performed in a steam atmosphere.

REGENERATION REACTION IN A NITROGEN ATMOSPHERE

Development of Analyzing Method

The spent carbons were fed continuously into the regeneration reactors, passing through three zones: drying, pyrolysis and carbonization, and gasification zones as stated earlier. First, the stage of the pyrolysis performed in an inert (nitrogen) atmosphere was considered.

The activated carbons used in the waste water treatment usually adsorbs various organic substances. Generally the pyrolysis of a single organic substance is represented by an irreversible first-order reaction. Therefore many first-order reactions are supposed to occur independently during the regeneration. The difference in the reaction rates is represented by the difference of activation energy, E, and frequency factor, k_0, if the rate equation of the Arrhenius type is assumed. Then the weight loss due to the pyrolysis of the j-th adsorbed species is represented by

$$-\frac{dq_j}{dt} = k_{0j}e^{-E_j/RT}q_j \tag{1}$$

where q_j is the residual amount adsorbed of the j-th adsorbate, E_j and k_{0j} are the activation energy and the frequency factor for the pyrolysis of the j-th adsorbate, respectively. If E_j, k_{0j} and the initial amount adsorbed, q_{0j}, were determined for each species, the total weight loss could be calculated by applying Eq. 1 to each species. However, not only the q_{0j} values but the number of adsorbed species is usually unknown. Therefore, it may be impossible to apply Eq. 1 to each species.

Pitt and Anthony et al. analyzed the rapid pyrolysis of coal based

on a model which assumes that the pyrolysis consists of a large number of first-order independent reactions. This method was originally derived by Vand. According to this method, the unconverted fraction of the volatiles during the pyrolysis is given as a function of time and temperature as

$$(V^* - V)/V^* = \int_0^\infty \exp\left[-k_0 \int_0^t e^{-E/RT}dt\right] f(E)dE \quad (2)$$

where V is the cumulative amount of volatiles evolved up to time t, V^* is the V value at $t \to \infty$, and $f(E)$ is the distribution function of activation energy defined so as to satisfy

$$\int_0^\infty f(E)dE = 1 \quad (3)$$

The weight change calculated by Eq. 2 was reported to be in good agreement with the experimental data in their analysis. In the analysis, however, the frequency factor, k_0, is represented by a typical value which was determined arbitrarily, though the frequency factors are supposed to be different for individual reactions. The distribution curve, $f(E)$, varies greatly depending on the selection of the k_0 value as shown later.

To overcome this weak point, the authors intended to correlate k_0 as a function of the activation energy, E, based on a well known experimental fact that the frequency factor increases with the increase of the activation energy for many chemical reactions including pyrolysis reactions. As a first approximation the following equation was employed:

$$k_0 = \alpha e^{\beta E} \quad (4)$$

where α and β are positive constants, and they are determined experimentally later. The relation of k_0 vs. E given by Eq. 4 is known as "compensation effect" in the field of chemical reaction kinetics.

With the modification for k_0, the relative residual amount of the adsorbed substances at the stage of pyrolysis of the thermal regeneration can be represented by

$$q^*(t) = \frac{q(t)}{q_0} = \int_0^\infty \exp\left[-\alpha e^{\beta E} \int_0^t e^{-E/RT}dt\right] f(E)dE \quad (5)$$

where q is the residual amount adsorbed and q_0 is the initial value of the amount adsorbed.

Equation 5 indicates that the weight loss of the spent carbon during the pyrolysis can be calculated when the relation between T and t are given, and α, β and $f(E)$ are predetermined.

Methods for Determining Distribution Curve

The distribution curve of the activation energy, $f(E)$, was determined by analyzing a thermogravimetric curve (TG curve) measured at a constant heating rate a. At the constant heating rate Eq. 5 is approximately rewritten to

$$q^*(T) \cong \int_0^\infty \Phi(E,T)f(E)dE \quad (6)$$

The function $\Phi(E,T)$ was approximated by

$$\Phi(E,T) \cong \exp\left[-\frac{\alpha e^{\beta E} T}{a} \cdot \frac{e^{-x}}{x}\right] \quad (7)$$

where $x = E/RT$.

By examining the change of $\Phi(E,T)$ with respect to E at fixed temperatures, $\Phi(E,T)$ was found to be approximated by the tangent line at the inflection point of $\Phi(E,T)$. Based on this approximation $f(E)$ was formulated approximately as follows:

$$f(\overline{E}) \cong -\frac{(1+w)^2}{R[u(u + W/u)(e/2 + w) + u(2w - u)]} \cdot \frac{dq^*}{dT} \quad (8)$$

where u, w, $\overline{E}$ and W are related to T, respectively, by the following equations.

$$u = E_{in}/RT \quad (9a)$$

$$w = E_{in}/RT - \beta E_{in} = u - \beta E_{in} \quad (9b)$$

TABLE 1. SPENT CARBONS USED FOR REGENERATION

Sample	Carbon Type	Liquid Being Purified
A	Coal (Takeda)	Municipal Waste Water
B	Coal (Calgon)	Municipal Waste Water
C	Coal (Fujisawa)	Waste Water of a Dye-Making Factory
D	Coal (Fujisawa)	Waste Water of a Chemical Factory

$$\overline{E} = \{(2w + e)/2(w + 1)\}E_{in} \quad (9c)$$

$$W = u(2 + u)/(1 + w) \quad (9d)$$

where E_{in} is the activation energy at the inflection point at Eq. 7, and is approximately related to T by

$$\frac{aE_{in}}{\alpha e^{\beta E_{in}} RT^2} \cong e^{-E_{in}/RT} \quad (10)$$

All the terms except dq^*/dT of the right hand side of Eq. 8 can be calculated beforehand for selected T values by use of Eqs. 9a, 9b, 9d and 10. The term dq^*/dT is obtained by differentiating graphically, or numerically, the TG curve measured at a constant heating rate a.

If $e/2$ is equated approximately to 1 in Eqs. 8 and 9c, Eq. 8 is reduced to a much simpler form:

$$f(E_{in}) \cong -\frac{1}{RW} \cdot \frac{dq^*}{dT} \quad (11)$$

This equation is also used to determine $f(E)$ later. The detailed derivation of Eqs. 8 and 10 are given in the Appendix.

If k_0 is represented by a typical value as was done so by Vand, Pitt and Anthony et al., Equations 8 and 11 are reduced to Eqs. 12 and 13, respectively:

$$f(\overline{E}) \cong -\frac{(1+u)^2}{R[u(u + U/u)(e/2 + u) + u^2]} \cdot \frac{dq^*}{dT} \quad (12)$$

$$f(E_{in}) \cong -\frac{1}{RU} \cdot \frac{dq^*}{dT} \quad (13)$$

where $U = u(2 + u)/(1 + u)$. Equation 13 coincides with the equation derived by Vand.

The procedure to evaluate $f(E)$ is put in order as follows:

(1) Measure a TG curve at a constant heating rate a, and plot q^* against T.

(2) Differentiate the TG curve at several T values to obtain dq^*/dT.

(3) Calculate E_{in}, u, w, $\overline{E}$ and W by use of Eqs. 9a to 10 at the selected T values.

(4) Insert E_{in}, u, w, $\overline{E}$, W and dq^*/dT into Eq. 8 or 11 to obtain $f(E)$. Use Eq. 12 or 13 instead of Eq. 8 or 11 if one approximately treats k_0 as constant.

EXPERIMENTAL

Spent Carbons Used

Four kinds of activated carbons employed in the waste water treatments were used to examine the method developed in this paper. The waste waters treated and the carbon types are given in Table 1. To determine the relation between k_0 and E, an activated carbon, CAL (Calgon Co.), which adsorbed known amounts of p-nitrophenol and a surface active agent (Emulgen 913, Kao-Atlas Co.), were used. The average particle diameters of the activated carbons were within 0.8 to 1.0 mm.

The activated carbons, CAL, of three different particle sizes were prepared, and almost the same amounts of dodecylbenzenesulfonate (DBS) were adsorbed onto them. These samples were used to investigate the effect of the intraparticle diffusion on the kinetics of the regeneration.

Experimental Apparatus

Figure 1 shows a schematic diagram of the experimental apparatus. The apparatus mainly consists of a reactor which is made of dual tube of quartz,

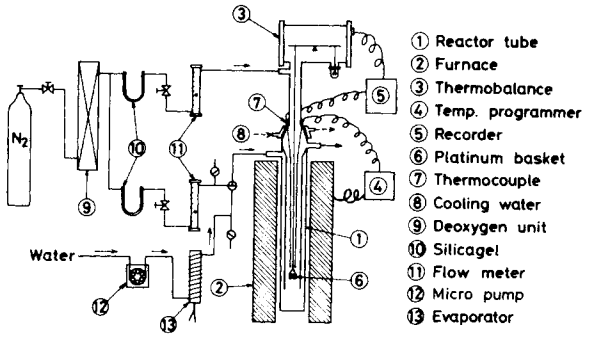

Figure 1. Schematic diagram of experimental apparatus.

a thermobalance, a temperature programmer by which the sample can be heated under any kind of heating patterns, and recorders.

Steam was generated in an evaporator made of a small tube packed with Raschig rings when the regeneration was performed under higher steam pressures (1.0, 0.5 and 0.25 atm). A nitrogen stream saturated with the distilled water was introduced into the reactor when lower steam pressures (0.12 and 0.06 atm) were employed. The temperature of the distilled water was carefully regulated to keep the steam pressure constant.

Sample particles were placed only in single layers on a basket made of platinum meshes to ensure good contact between gas and solid.

Experimental Procedure

A dried and carefully weighed sample (the weight was around 80 mg) was placed on the basket and was heated up to 120°C in a nitrogen atmosphere. After the weight of the sample reached a constant value, the sample was heated at a constant heating rate, or a predetermined heating profile, and the changes in the weight and the temperature were recorded.

The flow rate of nitrogen was 500 mL/min at S.T.P., which was large enough to neglect the mass transfer resistance at the particle surface. About 500 mL/min of nitrogen was also supplied from the upper side of the reactor to prevent thermobalance from the gases at higher temperatures.

When the regeneration was performed under a steam atmosphere, the water stuck to the basket if the steam was introduced at lower temperatures. Therefore, the nitrogen stream was gradually changed to a steam stream at 250°C, and was completely changed to the steam stream of the desired partial pressure at 300°C.

REGENERATION IN A NITROGEN ATMOSPHERE

Effect of Experimental Conditions

The TG curve must be obtained under the chemical reaction controlling regime to evaluate $f(E)$ by the proposed method. The mass transfer resistance at the particle surface was negligible at the flow rate of 500 mL/min (S.T.P).

Figure 2 shows the TG curves for DBS adsorbed onto the activated carbons of three different particle sizes. The amounts of DBS adsorbed were almost the same for the three carbons. No significant difference was found among the three TG curves, indicating that the intraparticle resistance is negligible for the particles smaller than 0.909 mm in diameter. The particle diameters of the spent carbons listed in Table 1 were about 0.8 to 1.0 mm, and the intraparticle diffusion resistance was supposed to be negligible for those carbons.

Relation between k_0 and E

Figure 3 shows the TG curve for Emulgen 913 adsorbed onto the activated carbon, CAL. If the pyrolysis reaction of Emulgen 913 is represented by a first order reaction, k_0 and E for this reaction can be determined by utilizing Eq. 1. The determined k_0 and E are given in Table 2. The solid line in Figure 3 is the TG curve calculated by using the predetermined k_0 and E. The calculated TG curve showed close agreement with the experimental data. Thus it was found that the pyrolysis of Emulgen 913 adsorbed onto the activated carbon can be represented by a first-order reaction.

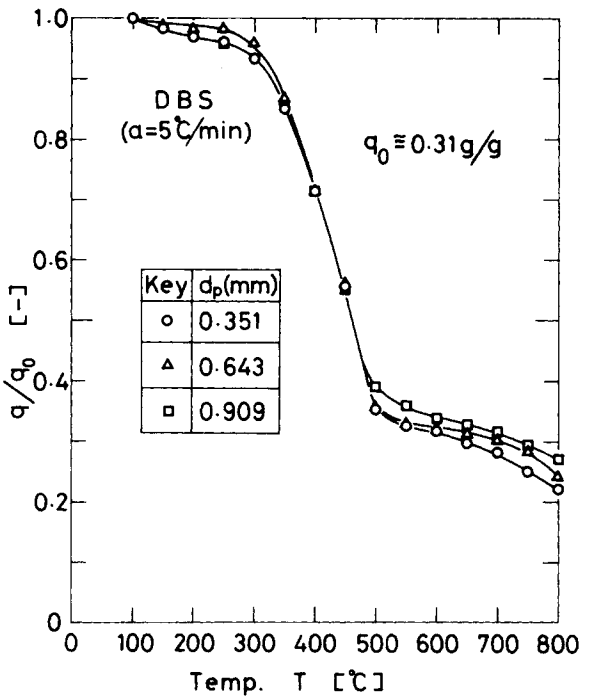

Figure 2. Effect of particle size on TG curve.

Similarly, k_0 and E were determined for the pyrolysis reactions of p-nitrophenol and glucose, respectively, and are given in Table 2. Here glucose was pyrolyzed without being adsorbed onto the activated carbon. In Table 2, k_0 and E for the pyrolysis reaction of DBS, which were obtained by Suzuki et al. (1978), are also given.

The k_0 values in Table 2 were plotted against E as shown in Figure 4. Clearly the frequency factor increases with the activation energy, and the following equation holds approximately:

$$k_0 = 10^3 e^{0.043E} \tag{14}$$

Thus, Eq. 4 was found to hold approximately in the pyrolysis reactions of organic substances adsorbed onto the activated carbons,

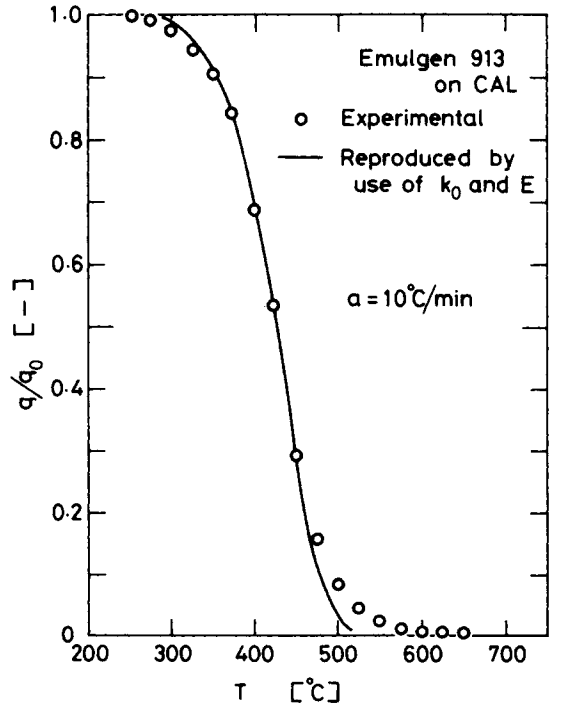

Figure 3. TG curve for Emulgen 913.

TABLE 2. ACTIVATION ENERGY AND FREQUENCY FACTOR FOR ORGANIC SUBSTANCES ADSORBED ON AN ACTIVATED CARBON

Sample	Activation Energy E [kJ/mol]	Frequency Factor k_0 [s^{-1}]
Emulgen 913	89.0	1.27×10^4
p-nitrophenol	74.4	8.57×10^3
Glucose[a]	92.0	1.20×10^5
DBS[b]	115	3.33×10^5

[a] This sample was pyrolyzed without being adsorbed.
[b] Values obtained by Suzuki et al. (1978).

and Eq. 4 can be used as a first approximation to the relation k_0 vs. E.

Determination of Activation Energy Distribution

TG curves were measured for four samples listed in Table 1 under a constant heating rate (a = 10°C/min). Figure 5 shows the TG curve for sample A. The shape of each of TG curves was slightly different among the samples, but only the result for sample A was shown to save space. Since the initial amounts adsorbed (q_0) were unknown for these spent carbons, the ordinate of Figure 5 represents $(1 + q)/(1 + q_0)$ which is the relative weight of the sample based on the initial weight including the activated carbon. Here it is assumed that the weight of the activated carbon remains constant during the regeneration in a nitrogen atmosphere.

The distribution curve can be obtained by inserting the derivatives of the TG curve in Figure 5, $q_0(dq^*/dT)/(q_0 + 1)$, instead of dq^*/dT into Eq. 8, but the distribution curve obtained in this manner is not $f(E)$ but $g(E)$ which is defined by

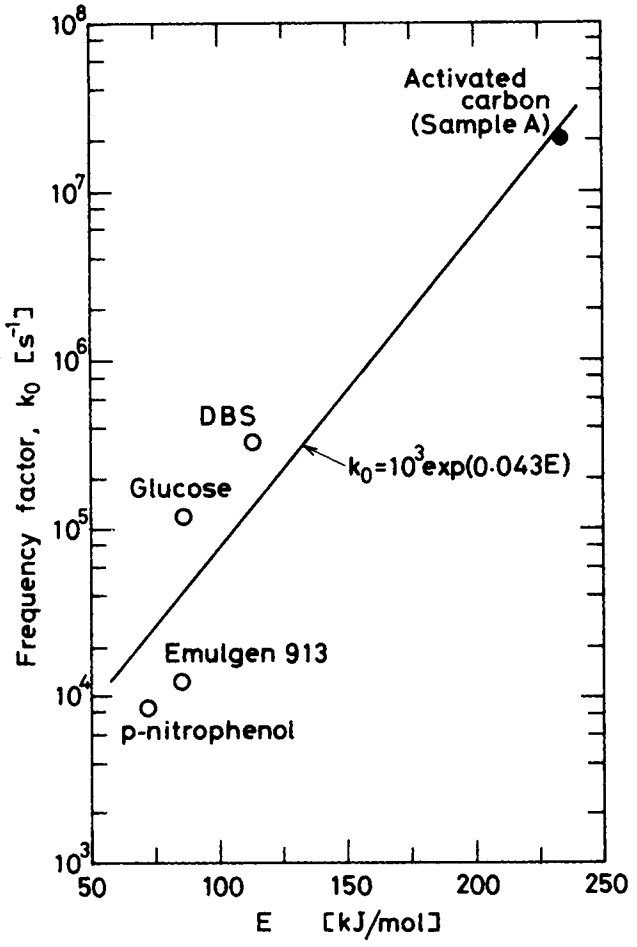

Figure 4. A correlation between k_0 and E.

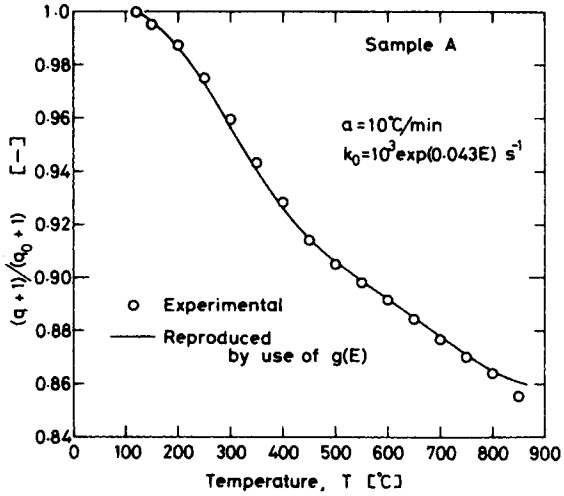

Figure 5. Comparison between reproduced and experimental TG curves (sample A).

$$g(E) = \frac{q_0}{q_0 + 1} f(E) \tag{15}$$

The solid line in Figure 6a shows the distribution curve $g(E)$ for sample A which was calculated by Eq. 8. The dotted line shows $g(E)$ calculated by Eq. 11. The solid and dotted lines almost coincide, indicating that no significant difference occurs between the distribution curve calculated by Eq. 8 and that by Eq. 11.

In Figure 6a the distribution curves calculated by assuming k_0 as constants are also shown for three cases ($k_0 = 10^4$, 10^7 and 10^{10} s^{-1}). These distribution curves were calculated by Eq. 12. The distribution curves change greatly depending on k_0, becoming less steep and moving toward the region of larger E values as k_0 increases. Since too large or too small activation energy is unlikely in the field of the pyrolysis of organic substances, and $g(E)$ should be determined uniquely for the pyrolysis under consideration, the treatment which assumes k_0 as a constant is not reasonable.

Figure 6b shows the distribution curves $g(E)$ calculated by use of Eq. 8 for samples B, C, and D.

Experimental *vs.* Calculated TG Curves

Since the distribution curves of the activation energy obtained for samples A, B, C and D were not $f(E)$ but $g(E)$, Eq. 5 must be modified to calculate the weight change of the samples. Inserting Eq. 15 into Eq. 5 and rearranging, results in the following equation:

$$\frac{q+1}{q_0+1} = \int_0^\infty \exp\left[-\alpha e^{\beta E} \int_0^t e^{-E/RT} dt\right] g(E)dE + \frac{1}{q_0+1} \tag{16}$$

The distribution curve $g(E)$, however, is obtained only within the range of 0 to E_{max} which is the E value obtained by inserting the maximum temperature of the measured TG curve into Eq. 10. Then the integrand of the right hand side (r.h.s.) is split into two terms at $E = E_{max}$ as

$$\frac{q+1}{q_0+1} = \int_0^{E_{max}} \exp\left[-\alpha e^{\beta E} \int_0^t e^{-E/RT} dt\right] g(E)dE + \int_{E_{max}}^\infty g(E)dE + \frac{1}{q_0+1} \tag{17}$$

where the term $\exp[-\alpha e^{\beta E} \int_0^t e^{-E/RT} dt]$ was eliminated from the second integrand of the r.h.s., because the term is almost unity for $E > E_{max}$. The sum of the last two terms in the r.h.s. of Eq. 17 produces a constant for each spent carbon, and can be determined by use of the TG curve which was utilized to determine $g(E)$. For a certain time t, the l.h.s. of Eq. 17 can be read from the TG curve, and the first term of the r.h.s. can be calculated by use of $g(E)$ determined. Then the sum of the last two terms of Eq. 17 can be

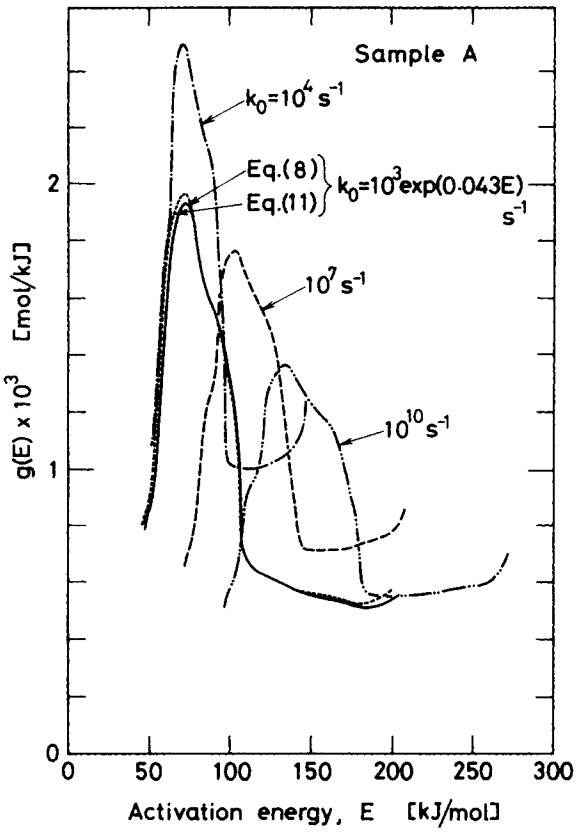

Figure 6a. Distribution curves of activation energy for the regeneration in a nitrogen atmosphere (sample A).

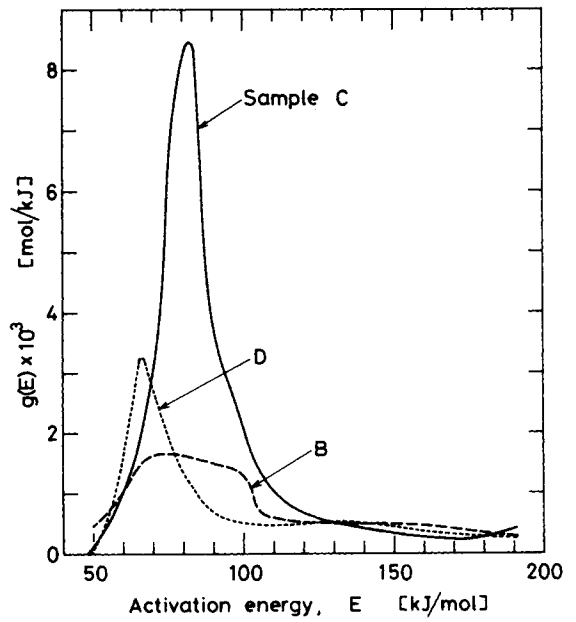

Figure 6b. Distribution curves of activation energy for the regeneration in a nitrogen atmosphere (samples B, C and D).

evaluated. Thus the relation $(q+1)/(q_0+1)$ vs. t is calculated by use of Eq. 17 when only the relation between T and t is given.

First, the TG curve for sample A, which was used to determine $g(E)$, was reproduced by use of the determined $g(E)$ (the solid line in Figure 6a) in order to examine whether the distribution curve $g(E)$ was correctly evaluated. The reproduced TG curve and the experimental data were in close agreement as shown in Figure 5, indicating that the distribution curve $g(E)$ was correctly evaluated. For samples B, C and D, the TG curves were also well reproduced by use of the determined distribution curves.

Next, the TG curves were purposely measured under a complicated heating profile as shown in Figure 7a. Furthermore, it was examined whether the TG curves could be predicted by use of the predetermined distribution curves. The TG curves can be calculated by inserting numerical values of $g(E)$ and the relation between T and t into Eq. 17, followed by numerical integration. The solid line in Figure 7a shows the predicted TG curve for sample A. The predicted TG curve and the experimental data showed close agreement. Figures 7b to 7d show similar comparisons for samples B, C and D. The predicted TG curves and the experimental data in these figures are also fairly good agreement. Thus, it was confirmed that the weight change accompanied by the pyrolysis under complicated heating conditions can be predicted well by the method developed in this paper.

As stated earlier, spent carbons are heated rather nonlinearly with time in continuous commercial regenerators. For designing regenerators it is required to predict the weight change of the spent carbons, namely the degree of the regeneration, under such heating conditions. The above discussion indicates that the proposed method is available for this requirement.

REGENERATION IN A STEAM ATMOSPHERE

Effect of Steam Pressure

Since steam is generally involved in the stream of the reactant gas, the analysis of the thermal regeneration in this steam atmosphere is of great importance for designing regenerators.

First, the effect of the steam pressure on the course of the regeneration was examined experimentally. Figure 8 shows the TG curves for sample A which were measured in six different steam pressures (1.0, 0.5, 0.25, 0.12, 0.06 and 0 atm). The ordinate of the figure is the relative weight normalized by the total initial weight. No significant difference was found among the TG curves at temperatures less than 450°C, but abrupt weight decrease occurred at temperatures greater than 700°C when steam was involved in the gas stream. These facts indicate that only the pyrolysis reaction occurs at temperatures less than 450°C and that the gasification by steam prevails at temperatures above 700°C. Therefore, the weight change of the sample can be calculated by the proposed method at temperatures less than 450°C, but the effect of gasification must be taken into account when the temperature exceeds 450°C.

Since the TG curves almost coincided when the steam pressure was greater than 0.12 atm, only the TG curve for the steam pressure of 1.0 atm was analyzed in the following sections.

Steam-Carbon Reaction

The reaction between steam and carbon has been studied by many investigators, and it is known that, in many cases, the weight change of the carbon is represented by the following equation:

$$-\frac{dW_c}{dt} = k_{c0}e^{-E_c/RT}W_c \qquad (18)$$

where W_c is the weight of the carbon, E_c and k_{c0} are, respectively, the activation energy and the frequency factor for the steam-carbon reaction.

The carbonized adsorbates as well as the activated carbon itself react with steam during the regeneration, but it is difficult to distinguish each contribution in the reactions of the two carbonaceous materials. Therefore, both reactions were assumed to have the same E_c and k_{c0}.

To prepare the sample which consists of the activated carbon and the carbonized adsorbates, sample A was heated to 980°C and was kept at that temperature for an hour in a nitrogen atmosphere. Then the sample was gasified with steam in the thermobalance at three different temperatures (785, 815 and 835°C). Figure 9 shows the change in relative weight of the sample. A linear relation holds between $ln(W_c/W_{c0})$ and t, indicating that Eq. 18 is valid. From

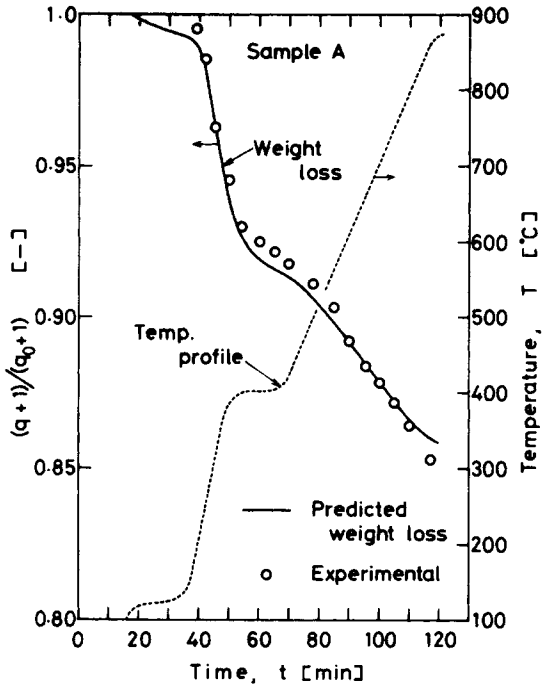

Figure 7a. Comparison between predicted and experimental TG curves under a nonuniform heating profile (nitrogen atmosphere, sample A).

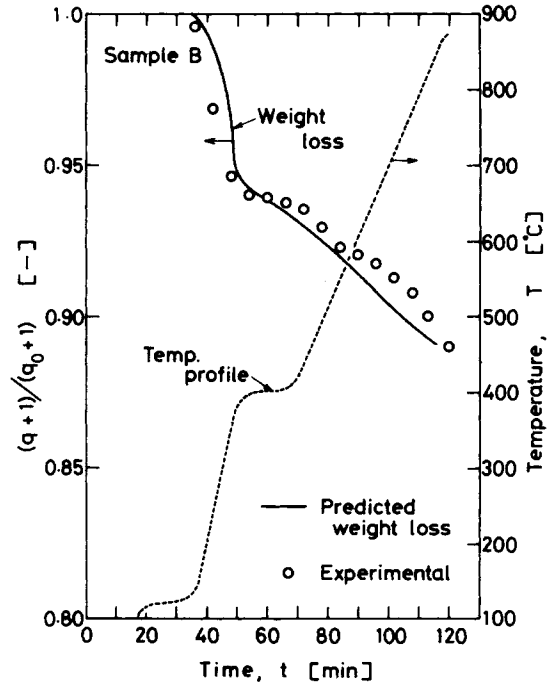

Figure 7b. Comparison between predicted and experimental TG curves under a nonuniform heating profile (nitrogen atmosphere, sample B).

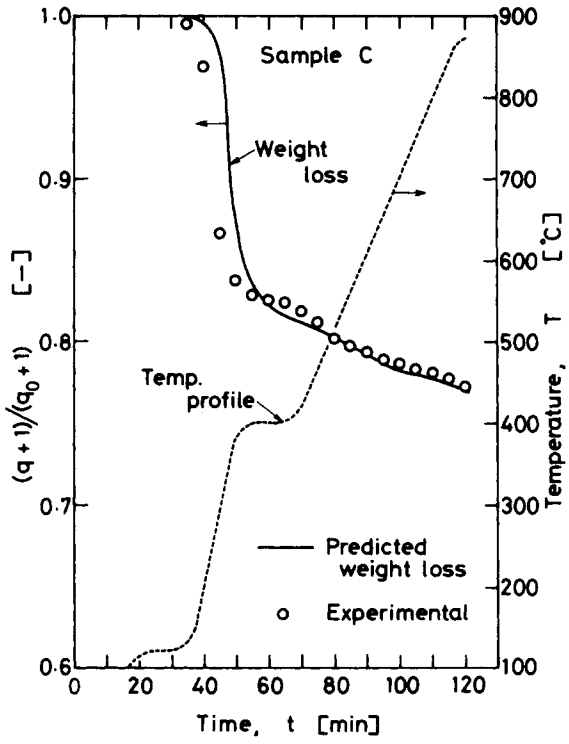

Figure 7c. Comparison between predicted and experimental TG curves under a nonuniform heating profile (nitrogen atmosphere, sample C).

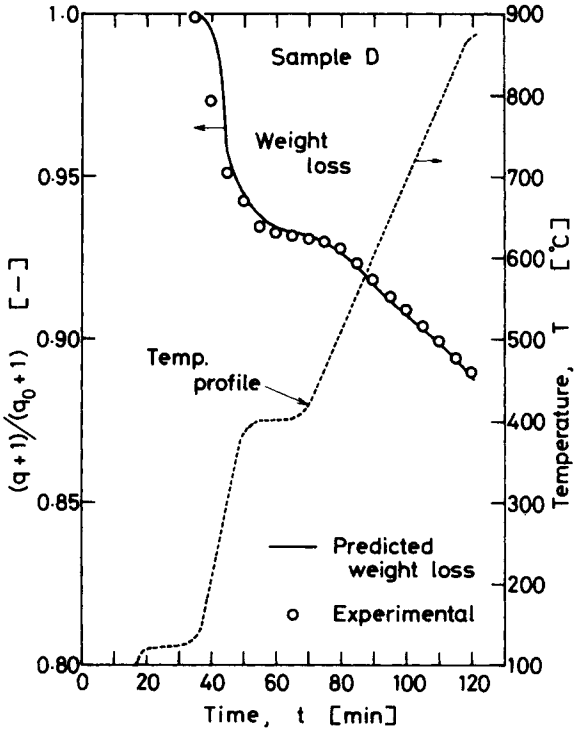

Figure 7d. Comparison between predicted and experimental TG curves under a nonuniform heating profile (nitrogen atmosphere, sample D).

this figure the values of $E_c = 233$ kJ/mol and $k_{c0} = 2.03 \times 10^7$ s^{-1} were obtained.

Equation 18 is the first-order with respect to W_c, and is analogous to Eq. 1. Then, the carbonaceous materials (the activated carbon and the carbonized adsorbates) may be regarded as an additional species of adsorbates, and the method originally developed for analyzing the pyrolysis may be applied to the whole regeneration stages including the gasification. In this case, Eq. 14 still holds as the relation between k_0 and E, because Eq. 14 was obtained including E_c and k_{c0} determined above.

Application to Regeneration in a Steam Atmosphere

The distribution curve of the activation energy can be obtained by inserting $d(W_t/W_{t0})/dT$ instead dq^*/dT into Eq. 6. The distribution curve obtained in this manner is represented by $G(E)$, and is related to the relative weight change of the sample as follows:

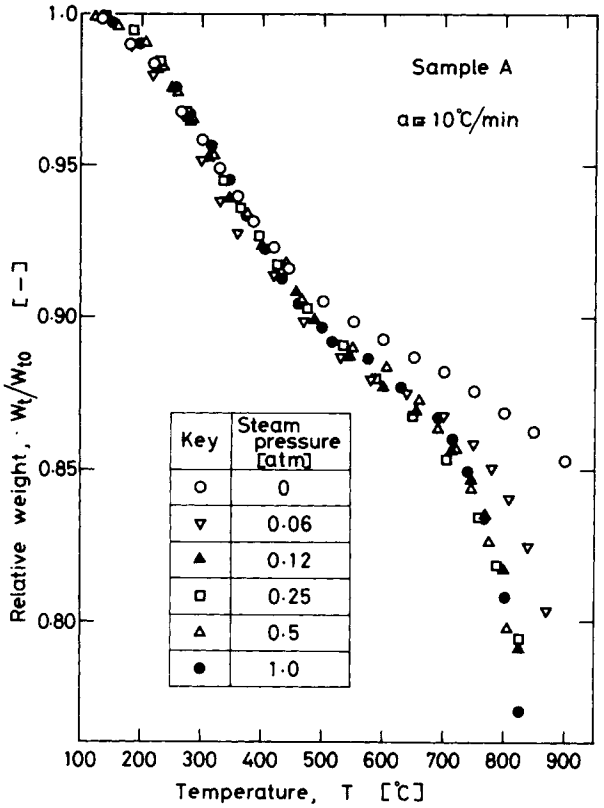

Figure 8. Effect of steam pressure on TG curve.

$$\frac{W_t}{W_{t0}} = \int_0^\infty \exp\left[-\alpha e^{\beta E}\int_0^t e^{-E/RT}dt\right]G(E)dE \qquad (19)$$

Figure 10 shows the distribution curve $G(E)$ for sample A. The abrupt increase of $G(E)$ at activation energies greater than 200 kJ/mol mainly corresponds to the gasification of the activated carbon and the carbonized adsorbates.

The TG curve was measured for sample A under the steam pressure of 1.0 atm and under the heating profile as shown in Figures 7a to 7d. Then the TG curve corresponding to this heating profile was predicted by inserting the predetermined $G(E)$ into Eq. 19, and is shown by the solid line in Figure 11. The predicted TG curve is in close agreement with the experimental data. This fact indicates that the method developed for analyzing the pyrolysis was also applicable to the analysis of the regeneration reaction performed in a steam atmosphere.

Thus it was found that the weight decrease of the spent carbon during the regeneration under a complicated heating profile can be closely predicted by the proposed method when a relation between k_0 vs. E and the distribution curve, $g(E)$ or $G(E)$, were predetermined. The proposed method is expected to be useful for designing regenerators.

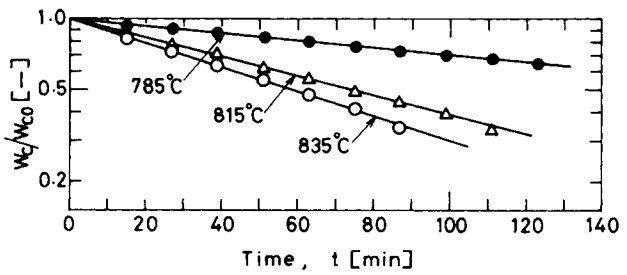

Figure 9. Reaction of the activated carbon and the carbonized adsorbates with steam.

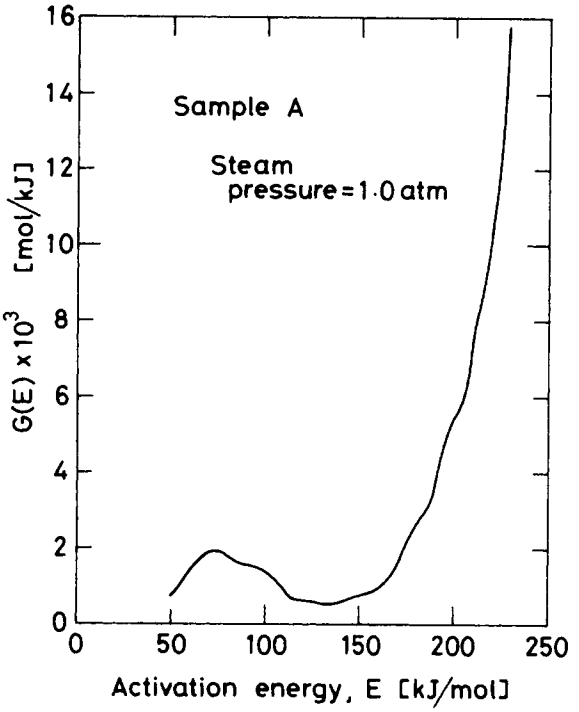

Figure 10. Distribution curve of activation energy for the regeneration in a steam atmosphere (sample A).

ACKNOWLEDGMENT

The authors are indebted to the Ministry of Education of Japan for the award of scientific research funds (Grant Nos. 555383 and 475729), and to the Takeda Research Fund for the donation of a research fund.

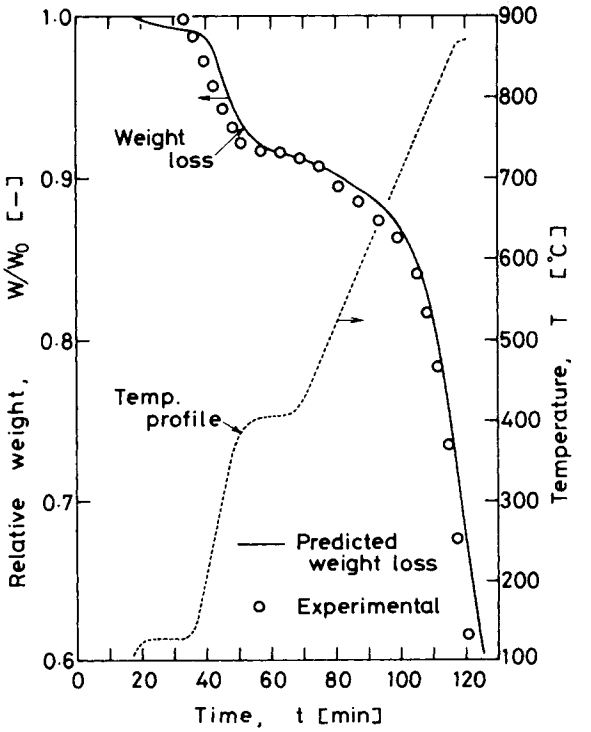

Figure 11. Comparison between predicted and experimental TG curves under a nonuniform heating profile (steam atmosphere, sample A).

APPENDIX: DERIVATION OF EQS. 8 AND 10

When the temperature of the sample is raised from T_0 at the constant heating rate of a, T is represented as

$$T = T_0 + at \tag{A1}$$

Substituting Eq. A1 into Eq. 5 gives

$$q^*(T) = \int_0^\infty \exp\left[-\frac{\alpha e^{\beta E}}{a}\int_{T_0}^{T} e^{-E/RT}dT\right] f(E)dE \tag{A2}$$

Since the TG curve is usually measured from lower temperatures under which the reaction does not occur, T_0 in Eq. A2 is approximately set equal to 0. Then

$$q^*(T) \cong \int_0^\infty \Phi(E,T)f(E)dE \tag{A3}$$

where $\Phi(E,T)$ is defined by

$$\Phi(E,T) = \exp\left[-\frac{\alpha e^{\beta E}}{a}\int_0^T e^{-E/RT}dT\right] \tag{A4}$$

The values of $\Phi(E,T)$ varies only between 0 and 1. By noting that $x = E/RT$, Eq. A4 is rewritten as follows:

$$\Phi(E,T) = \exp\left[-\frac{\alpha e^{\beta E}E}{aR}\left(\frac{e^{-x}}{x} - \int_x^\infty \frac{e^{-x}}{x}dx\right)\right]$$

$$= \exp\left[-\frac{\alpha e^{\beta E}E}{aR}p(x)\right] \tag{A5}$$

To find an approximate expression for $\Phi(E,T)$, the change of $\Phi(E,T)$ with respect to E was examined at fixed temperatures. The solid line in Figure A-1 shows a typical relationship between $\Phi(E,T)$ and E calculated by Eq. A5, in which T is fixed at 573.15 K, and k_0 and a are selected as $10^3e^{0.043E}$ s^{-1} and 10°C/min, respectively.

By employing an approximation $p(x) \cong e^{-x}/x^2$, which is frequently used, Eq. A5 is reduced to

$$\Phi(E,T) \cong \exp\left(-\frac{\alpha e^{\beta E}T}{a}\cdot\frac{e^{-x}}{x}\right) \tag{A6}$$

The broken line in Figure A-1 was calculated by this equation. Since the broken line almost coincides with the solid line, Eq. A6 was employed in the analysis instead of the complicated Eq. of A5.

The broken line in Figure A-1 changes sharply against E. This indicates that Eq. A6 may be further approximated by the tangent line at the inflection point. To obtain the activation energy, E_{in}, at the inflection point of Eq. A6 at a fixed temperature, Eq. A6 was differentiated with E twice as

$$\frac{\partial^2\Phi}{\partial E^2} = \frac{\alpha e^{\beta E}}{aR^2T}\cdot\frac{e^{-x}}{x}\Phi\left\{\left(1+\frac{1}{x}-\beta RT\right)^2 \times\left(\frac{\alpha e^{\beta E}RT^2}{aE}e^{-x}-1\right)-\frac{1}{x^2}\right\} \tag{A7}$$

Since $\partial^2\Phi/\partial E^2 = 0$ holds at the inflection point $E = E_{in}$, E_{in} is calculated from the following transcendental equation

$$\left(1+\frac{RT}{E_{in}}-\beta RT\right)^2\left(\frac{\alpha e^{\beta E_{in}}RT^2}{aE_{in}}e^{-E_{in}/RT}-1\right)-\frac{R^2T^2}{E_{in}^2}=0 \tag{A8}$$

After examining the behavior of Eq. A8, it was found that the last term may be omitted and that the term $1 + RT/E_{in} - \beta RT$ is greater than zero. Therefore E_{in} is calculated from a simpler equation as

$$\frac{aE_{in}}{\alpha e^{\beta E_{in}}RT^2} \cong e^{-E_{in}/RT} \tag{A9}$$

This is Eq. 10 shown in the text. To examine the accuracy of Eq. A9, the E_{in} values calculated by Eq. A9 was compared with those calculated by Eq. A8. For a = 10°C/min, $\alpha = 10^3$s^{-1}, β = 0.043 mol/kJ and T = 100 to 850°C, the relative errors between the above two E_{in}'s were less than 0.05 %. This indicates that Eq. A9 may be employed with good accuracy to calculate E_{in} for a specified temperature T.

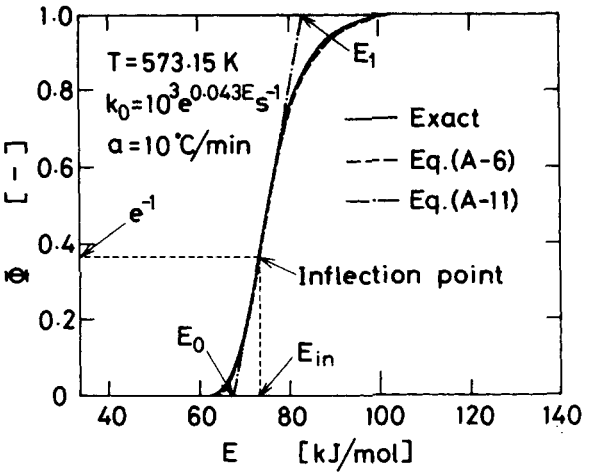

Figure A-1 Relation of $\Phi(E,T)$ vs. E.

The value of Φ at $E = E_{in}$ is calculated by inserting Eq. A9 into A6 as

$$(\Phi)_{E=E_{in}} = 1/e = 0.3678\ldots \tag{A10}$$

It is noted that this equation holds irrespective of the temperature. Then the tangent line at the inflection point of Eq. A6, namely an approximate expression for $\Phi(E,T)$, is represented by

$$\Phi(E,T) \cong \left(\frac{\partial\Phi}{\partial E}\right)_{E=E_{in}}(E-E_{in}) + 1/e = A(T)E + B(T) \tag{A11}$$

where $A(T)$ and $B(T)$ are related to T through E_{in} as follows:

$$A(T) = \left(\frac{\partial\Phi}{\partial E}\right)_{E=E_{in}} = (w+1)/eE_{in} \tag{A12}$$

$$B(T) = -\left(\frac{\partial\Phi}{\partial E}\right)_{E=E_{in}}E_{in} + 1/e = -w/e \tag{A13}$$

Substituting Eq. A11 into Eq. A3, and differentiating the resulting equation with respect to T gives

$$\frac{dq^*}{dT} = \frac{dA}{dT}\int_{E_0}^{E_1} Ef(E)dE + \frac{dB}{dT}\int_{E_0}^{E_1} f(E)dE \tag{A14}$$

where E_0 and E_1 are the values of E at which Eq. A11 intersects with $\Phi(E,T) = 0$ and 1, respectively, and are represented by

$$E_0 = \frac{w}{w+1}E_{in} \tag{A15}$$

$$E_1 = \frac{w+e}{w+1}E_{in} \tag{A16}$$

The terms dA/dT and dB/dT are obtained from Eqs. A12 and A13, respectively. Since w is larger than 10 and E_{in} may be 230 kJ/mol at its largest, the difference between E_0 and E_1 is generally around 20 kJ/mol, which is much smaller than the variable range of the distribution curve $f(E)$. This allows one to adopt the following approximations:

$$\int_{E_0}^{E_1} Ef(E)dE \cong \bar{E}(E_1-E_0)f(\bar{E}) \tag{A17}$$

$$\int_{E_0}^{E_1} f(E)dE \cong (E_1-E_0)f(\bar{E}) \tag{A18}$$

where $\bar{E}$ was defined by

$$\bar{E} = (E_0+E_1)/2 = \frac{2w+e}{2(w+1)}E_{in} \tag{A19}$$

Then substitution of Eqs. A17 and A18 into Eq. A14, and rearrangement of the resulting equation finally gives

$$f(\bar{E}) \cong -\frac{(1+w)^2}{R[u(u+W/u)(e/2+w)+u(2w-u)]} \cdot \frac{dq^*}{dT} \tag{A20}$$

Thus, Eq. 8 was obtained.

NOTATION

a = heating rate, °C/min, K/s
d_p = particle diameter, mm
E = activation energy, kJ/mol
E_c = activation energy for steam-carbon reaction, kJ/mol
E_{in} = E value at inflection point of Φ function, kJ/mol
E_j = E value for j-th species of adsorbates, kJ/mol
E_{max} = E value obtained by inserting a maximum temperature of TG curve into Eq. 10, kJ/mol
E_0 = activation energy defined by Eq. A14, kJ/mol
E_1 = activation energy defined by Eq. A15, kJ/mol
$\bar{E}$ = $(E_0 + E_1)/2$, kJ/mol
$f(E)$ = distribution curve of activation energy, mol/kJ
$G(E)$ = distribution curve of E for the regeneration reaction in a steam atmosphere, mol/kJ
$g(E)$ = Distribution curve of E defined by Eq. 15, mol/kJ
k_{c0} = frequency factor for steam-carbon reaction, s^{-1}
k_0 = frequency factor, s^{-1}
k_{0j} = k_0 value for j-th species of adsorbates, s^{-1}
$p(x)$ = $e^{-x}/x - \int_x^\infty (e^{-x}/x)dx$
q = residual amount adsorbed at t, g/g-carbon
q_j = q value for j-th species, g/g-carbon
q_0 = q value at $t = 0$, g/g-carbon
q^* = q/q_0
R = gas constant, 8.314 J/mol·K
T = temperature, °C, K
t = time, min, s
U = $u(2+u)/(1+u)$
u = E_{in}/RT
V = cumulative amount of volatiles evolved
V^* = V value at $t \to \infty$
W = $u(2+u)/(1+w)$
W_c = weight of carbon at t, g
W_{c0} = W_c value at $t = 0$, g
W_t = total weight of sample at t, g
W_{t0} = W_t value at $t = 0$
w = $E_{in}/RT - \beta E_{in}$
x = E/RT

Greek Letters

α = constant in Eq. 4, s^{-1}
β = constant in Eq. 4, mol/kJ
Φ = function defined by Eq. A5

LITERATURE CITED

Anthony, D. B., J. B. Howard, H. C. Hottel, and H. P. Meissner, "Rapid Devolatilization of Pulverized Coal," 15th Symp. on Combustion, p. 1303, The Combustion Institute, Pittsburgh, PA (1975).

Hashimoto, K., K. Miura, T. Yamanishi, and T. Yamane, "Thermal Regeneration of Activated Carbons used in Waste Water Treatment," AIChE Meeting, No. 122C, San Francisco (Nov., 1979).

Hutchins, R. A., "Economic Factors in Granular Carbon Thermal Regeneration," *Chem. Eng. Prog.*, **69**, No. 11, 48 (1973).

Kawazoe, K., and T. Osawa, "Pore-volume Change with Thermal Regeneration of Spent Activated Carbon," *Kogyo Yosui* (Industrial Water), No. 248, 17 (1979).

Loven, A. W., "Perspectives on Carbon Regeneration," *Chem. Eng. Prog.*, **69**, No. 11, 56 (1973).

Pitt, G. J., "The kinetics of the Evolution of Volatile Products from Coal," *Fuel*, **41**, 267 (1962).

Suzuki, M., D. M. Misic, O. Koyama, and K. Kawazoe, "Study of Thermal Regeneration of Spent Activated Carbons," *Chem. Eng. Sci.*, **33**, 271 (1978).

Urano, K., "Regeneration of Activated Carbon used for Sewage Treatment," *Nippon-Kagaku-Kaishi*, No. 5, 975 (1972).

Vand, V., "A Theory of the Irreversible Electrical Resistance Changes of Metallic Films Evaporated in Vacuum," Proc. Phys. Soc. (London), A55, 222 (1942).

Manuscript received October 9, 1980; revision received September 17, and accepted October 13, 1981.